Resistive Switching in Ferromagnetic $La_{2/3}Ca_{1/3}MnO_3$ Thin Films

I. Alposta[1], A. Kalstein[1,2], N. Ghenzi[1,2], S. Bengio[2,3], G. Zampieri[2,3], D. Rubi[1,2,4], and P. Levy[1,2]

[1]Centro Atómico Constituyentes (CNEA), San Martín, Buenos Aires, Argentina
[2]Consejo Nacional de Investigaciones Científicas y Técnicas (CONICET), Argentina
[3]Centro Atómico Bariloche (CNEA), S. C. de Bariloche, Río Negro, Argentina
[4]Escuela de Ciencia y Tecnología, UNSAM, San Martín, Buenos Aires, Argentina

Ferromagnetic thin films of $La_{2/3}Ca_{1/3}MnO_3$ manganite were grown by pulsed laser deposition, under different oxygen atmospheres, on silicon substrates. We performed structural, magnetic, spectroscopic, and electrical characterization of the films. Resistive switching between high and low resistance states was obtained upon pulsing with opposite polarities voltages. The *I-V* curves exhibit sharp transitions between these states. The RS properties are strongly dependant on the films oxygen stochiometry and on the compliance current used for producing the high to low transition. ON/OFF ratios as high as 1000 were obtained for optimal RS conditions. Obtained results are discussed within the framework of mobile oxygen vacancies.

***Index Terms*—Ferromagnetism, manganites, RRAM memories, thin films.**

I. Introduction

SEVERAL simple and complex oxides display electrical field induced resistance switching (RS), i.e. the reversible change of their resistance state by applying voltage or current pulses of a few ns [1]–[3]. This type of switching presents low power consumption, which combined with other advantages like high retention times, high endurance and good temperature stability, turn these materials into potentially good candidates to be used for resistive random access memory (ReRAM) technology [4].

A typical RS device consists of an insulating or semiconductor oxide sandwiched between two metallic electrodes. According to the switching behavior, RS can be classified in two main categories. In unipolar switching, high-to-low and low-to-high resistance change (SET and RESET processes, respectively) can be achieved by applying pulses of the same polarity (either positive or negative). In contrast, in bipolar switching different polarities are needed to SET and RESET the device. Switching in simple oxides is usually reported as unipolar and related with the formation/rupture of nanofilaments connecting both electrodes. On the other hand, bipolar switching is frequently found in complex oxides and related to an interface mechanism associated with the movement of oxygen vacancies near the metal-oxide interface. However, the previous classification (simple oxides-filamentary RS and complex oxides-interface RS) is not fully consistent with all reported systems and exceptions are found in the literature [5].

Perovskite manganites with general formula $ReAMnO_3$ (Re: rare earth ions, A: alkaline ions) have been the subject of extensive studies in the past years due to their complex and intermixed structural, electronic, magnetic, and transport properties, being the colossal magnetoresistance (CMR) the most celebrated property [6], [7]. In addition, after the initial report by Ignatiev *et al.* [8] on $Pr_{0.7}Ca_{0.3}MnO_3$ thin films, many studies regarding the RS behavior of both ceramics and thin films of different manganites have been performed [9]–[12]. Moreover, successful models that explain nontrivial features of *I-V* curves of manganites displaying RS have been developed [13], [14].

In this paper, we describe how we grew and characterized thin films of the canonical $La_{2/3}Ca_{1/3}MnO_3$ manganite with different oxygen content. Structural, magnetic, spectroscopic, and electrical characterizations have been performed. We have found that their RS behavior is strongly dependant on the oxygen stochiometry of the films. We have also found a dependence of the R_{HIGH}/R_{LOW} ratio with the SET compliance current (CC), obtaining figures of up to 1000 for optimum oxygen content and SET CC.

II. Experimental Procedure

We grew 100 nm $La_{2/3}Ca_{1/3}MnO_3$ (LCMO) manganite thin films by pulsed laser deposition (pulsed Q-switched Spectra Physicas Laser with $\lambda = 355$ nm and a frequency of 10 Hz) at different oxygen pressures ranging from 0.05 to 0.35 mbar and at a fixed temperature of 680 °C. The LCMO target was prepared by pressing at 10 Tons fine powders prepared by the liquid mix method. After pelletizing, the target was sintered at 1400 °C for 2 h. Films were grown on top of highly conductive n-type silicon, which also acted as bottom electrode. We used hand-painted Ag as top electrodes, with areas around 1 mm^2. Structural characterization was performed by X-ray diffraction (XRD) by means of an Empyrean (Panalytical) diffractometer in standard $\omega - 2\theta$ configuration. The surface of the films was studied by scanning electron microscopy (SEM) by means of a FEI Quanta 200 microscope. Magnetic characterization was performed with a Versalab (Quantum Design) magnetometer. We also performed X-ray photoemission spectroscopy (XPS) at room temperature by means of a spectrometer with a hemispherical electrostatic energy analyzer ($r = 10$ cm) using an Al K_α radiation source ($h\nu = 1486.6$ eV). The electrical characterization was performed with a Keithley 2612 hooked to a probe station. The acquisition software was programmed on the LabView environment.

Manuscript received February 15, 2013; revised March 22, 2013; accepted April 09, 2013. Date of current version July 23, 2013. Corresponding author: D. Rubi (e-mail: rubi@tandar.cnea.gov.ar).

Color versions of one or more of the figures in this paper are available online at http://ieeexplore.ieee.org.

Digital Object Identifier 10.1109/TMAG.2013.2258662

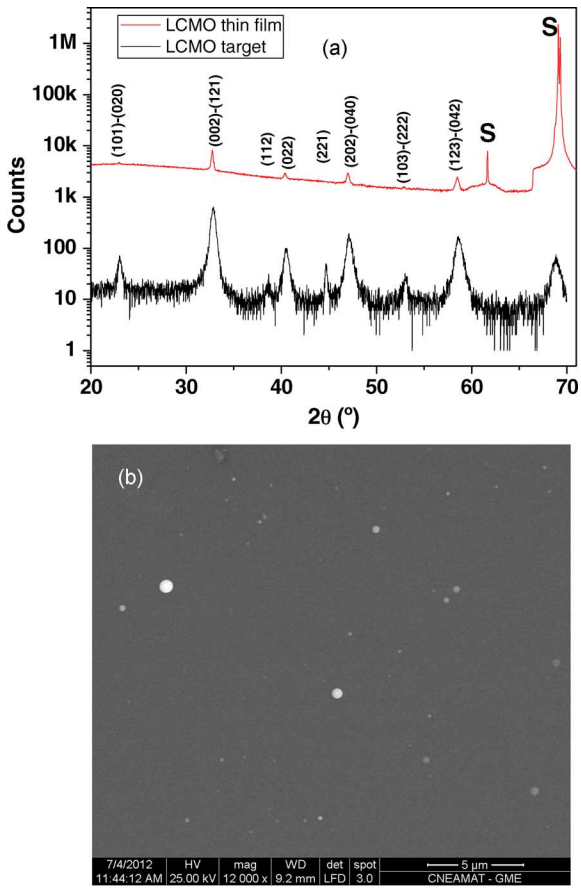

Fig. 1. (a) XRD spectrum corresponding to both the LCMO target (black line) and a thin film (red line) grown at 0.13 mbar. (b) SEM image corresponding to an LCMO thin film.

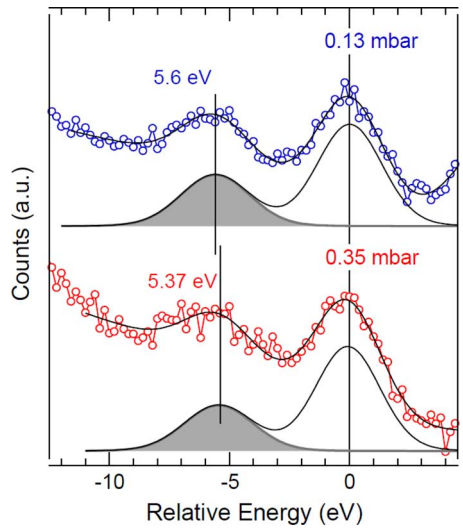

Fig. 2. XPS Mn-3s spectra corresponding to LCMO thin films grown at oxygen pressures of 0.13 and 0.35 mbar. Open symbols are the experimental data while black lines correspond to the fittings.

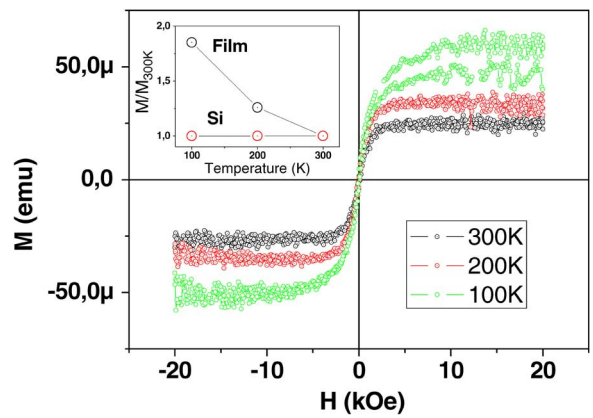

Fig. 3. Magnetization as a function of the magnetic field at different temperatures for a LCMO thin film grown at 0.13 mbar of O_2. Diamagnetic contribution from the substrate was discounted. Inset shows the evolution with the temperature of the normalized (300 K) saturation magnetization for the same film and for a bare Si substrate.

III. Results and Discussion

Fig. 1(a) shows the XRD spectra corresponding to both the LCMO target (black line) and a LCMO thin film (red line) grown at an oxygen pressure of 0.13 mbar. The XRD peaks were indexed according to the *Pnma* space group. The film resulted single phase and polycrystalline. No particular texture was found, which is a consequence of the presence of the amorphous native SiO_x layer at the Si surface, that prevents textured or epitaxial growth. The SEM image of Fig. 1(b) shows an homogeneous surface with the presence of a moderate amount of submicrometric particulate on the surface of the film, which is usually found in films grown by pulsed laser deposition [15].

In order to test the Mn valence state (and therefore estimate the oxygen content) of the films, we have measured the Mn-3s X-ray photoemission spectra (XPS) of films grown at different oxygen pressures. As the Mn-3s level displays an energy splitting originated by the intra-atomic exchange coupling between 3s and 3d electrons, the magnitude of the splitting has been proposed to be proportional to the local Mn valence [16]. Fig. 2 shows the obtained spectra for films grown at 0.13 and 0.35 mbar oxygen pressures. The respective Mn-3s splittings are 5.6 and 5.37 eV, respectively, indicating formal Mn valences of $+2.7$ and $+3$ [16]. The corresponding calculated oxygen stochiometries are $\sim$2.68 and $\sim$2.83, respectively. This clearly shows that reducing the growth oxygen pressure lowers the Mn valence and creates oxygen vacancies.

Fig. 3(a) shows magnetic hysteresis loops recorded at different temperatures for a film grown at 0.13 mbar. The ferromagnetic response, which increases as the temperature decreases, is evident. It is worth noting that magnetic measurements in thin films imply very weak signals that could be masked by the presence of magnetic contaminants acquired during the manipulation of the sample (indeed, we verified in a piece of bare Si a weak ferromagnetic response). These magnetic impurities are basically ferromagnetic Fe and exhibit a Curie temperature well above room temperature, so their saturation magnetization (M_S) displays little variation below room temperature. The inset of Fig. 3 displays the evolution of M_S normalized to the corresponding value at 300 K $(M_{S,300\,K})$ for the same film and for a control experiment on a bare Si substrate. It is clear that the latter presents no changes upon cooling while the former increases, thus indicating that we are indeed decoupling the magnetic signal arising from the thin oxide layer. Magnetization as a function of the temperature measurements (not shown here) suggest that the Curie temperature in this oxygen deficient film is around 210 K,

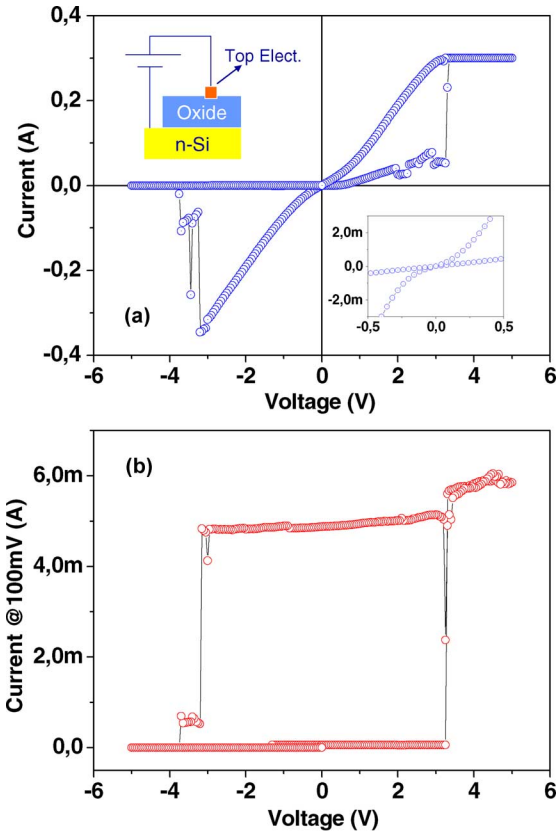

Fig. 4. (a) Pulsed *I-V* curve for an n-Si/LCMO/Ag device, using CC $=$ 300 mA for the SET step. Left inset depicts the electrode configuration and polarities; right inset is enlargement of the same curve at low voltages. (b) Hysteresis switching loop for the same device using a bias of 100 mV applied after each voltage pulse.

which is lower than the bulk, stochiometric compound, value (∼270 K). This depleted T_C may be related to the presence of oxygen vacancies, which induce a "self-doping" effect [17] that weakens the magnetic interaction.

We will focus now on the electrical characterization. We have recorded simultaneously, at room temperature, pulsed *I-V* curves and hysteresis switching loops (HSL) [18]. The pulsed *I-V* curve consists of applying a sequence of voltage pulses of different amplitudes ($0 \rightarrow 5$ V $\rightarrow 0 \rightarrow -5$ V $\rightarrow 0$, with a time-width of the order of a few milliseconds and a step of 50 mV) while the current is measured *during* the application of the pulse. We remark that this is a dynamic measurement. In addition, after the application of each of these pulses we apply a small reading voltage of 100 mV that allows us to measure the current and evaluate the *remnant* resistance state (HSL). The inset of Fig. 4 depicts the electrode configuration and polarities. Fig. 4(a) and (b) shows a pulsed *I-V* curve and the corresponding HSL for a LCMO sample grown at an oxygen pressure of 0.13 mbar. Fig. 4(a) shows that the device is initially in a high resistance (low current) state. As the voltage is increased, the current remains low up to a value of ∼3.5 V, where one can see an abrupt jump to a high current state, reflecting the transition of the device from high to low resistance, in what is usually called the SET process. A CC is externally programmed to avoid device damage during the SET. We recall that after the SET process the source automatically adjusts the voltage to reach that limiting current. In consequence, a lower voltage than the nominal one is really applied. When the voltage is decreased the system remains in the low resistance state until a negative voltage of ~ -3 V is reached, where there is a sudden current drop, reflecting the transition from low to high resistance. This is what is called the RESET process. The fact that the SET process takes place for positive voltages while the RESET occurs for negative voltages shows that we are dealing with *bipolar* resistive switching, as is usually found for complex oxides. Fig. 4(b) shows the HSL corresponding to the same measurement. The high and low resistance states are clearly defined with abrupt transitions, displaying values of ~ 10 kΩ and ~ 20 Ω, respectively. The bipolar switching in complex oxides is usually related to the electrical field induced movement of oxygen vacancies near the electrode/oxide interface. According to this scenario, the application of electrical pulses modifies the oxygen vacancies profile close to the metal-insulator interface [13], [14], changing its resistance. For instance, a negative voltage applied to the top Ag electrode induces the migration of positively charged oxygen vacancies from the "bulk" to the metal-oxide interface. The number of vacancies is thus increased near the interface, disrupting Mn-O-Mn bonds (associated to the electronic transport in manganites) and resulting in an increase of the junction resistance (high resistance state). The application of a positive voltage induces the movement of oxygen vacancies from the interface to the "bulk", increasing the number of Mn-O-Mn paths near the interface and leading to a low resistance state. In our case, it is worth remarking that we are measuring the electrical properties in a transversal configuration (n-Si/LCMO/Ag) and we therefore have two interfaces in series that may show a complementary behavior if they are both active [13]. In those cases, the HSL displays complex shapes such as the so-called "table with legs" [14]. However, we see in our case that the HSL displays a squared shape, strongly indicating that we have only one active interface (presumably LCMO/Ag, as extensively reported in the literature [19], [20]) while the other interface (n-Si/LCMO) does not switch at all. The inset of Fig. 4(a) is an enlargement of the *I-V* curve for low voltages and shows a linear (nonlinear) behavior for the high (low) resistance state, suggesting different conduction mechanisms for both resistance states.

In order to obtain devices for applications, it is desirable to obtain ON/OFF (or equivalently R_{HIGH}/R_{LOW}) ratios as large as possible. We found that this ratio is extremely dependant on the SET CC; Fig. 5 shows the evolution of R_{HIGH}/R_{LOW} as a function of the SET compliance current and the oxygen content. For films grown at 0.05 and 0.13 mbar, it is found that the ratio first increases as CC increases, reaching a maximum of ∼1000 for CC ∼100 mA. In this regime, increasing the SET CC produces a lowering of R_{LOW} (not shown here), while R_{HIGH} remains nearly constant. On the other hand, for CCs above 100 mA, R_{HIGH} starts to drop pronouncedly, lowering the R_{HIGH}/R_{LOW} ratio two orders of magnitude.

For low CCs, the increase of the SET maximum current determines a concomitant increase on the total amount of vacancies depleted from the interfacial region. Preliminary simulations using the Vacancy Enhanced Oxygen Vacancies drift [14] support this picture.

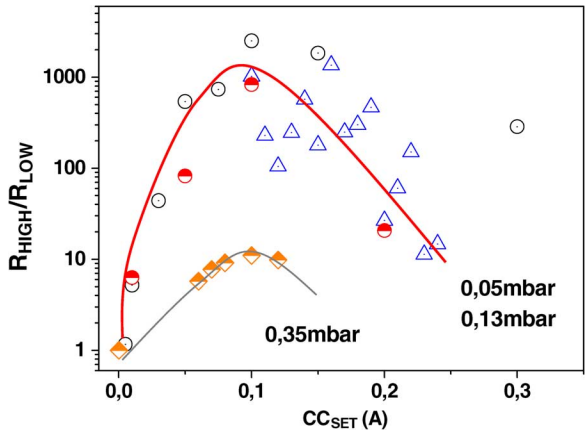

Fig. 5. Evolution of the R_{HIGH}/R_{LOW} ratio as a function of the SET compliance current for different LCMO thin films grown at 0.05, 0.13, and 0.35 mbar of O_2.

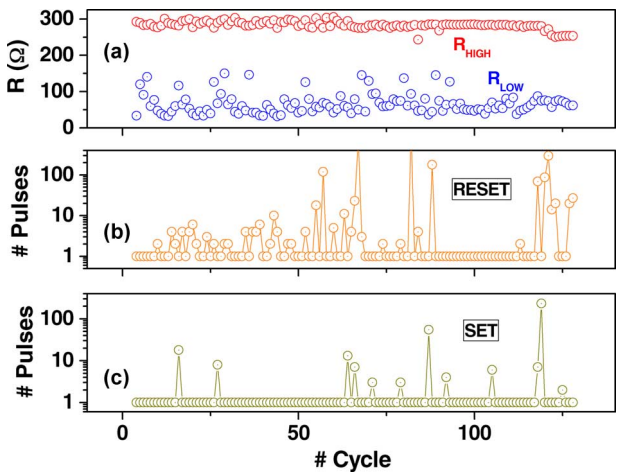

Fig. 6. (a) High and low resistance states obtained by accumulating pulses of 4 V (SET) and −5 V (RESET) until the switching takes place. (b), (c) Number of pulses needed to RESET and SET the resistive state during each cycle.

The behavior found at higher CCs may be related to a crossover to a filamentary regime (to be reported elsewhere). The filamentary regime implies the formation of a metallic nano-filament (associated to metal diffusion into the oxide) connecting both electrodes. This filament can be "burned" by Joule effect and the sample can be RESETED, so in principle and for the compliances showed in Fig. 5 the behavior is reversible. For higher compliances, after the SET process, the sample remains in a low resistance state and can not be further RESETED.

It is also worth noting from Fig. 5 that the electrical response is severely reduced upon increasing the oxygen pressure during the growth. Indeed, the film grown at 0.35 mbar displays a maximum R_{HIGH}/R_{LOW} ratio of only ∼10. This clearly shows that the presence of oxygen vacancies (as determined by the XPS experiments already described) plays a crucial role in the RS behavior. On the contrary of what is desired for magnetic properties optimization, oxygen off-stochiometries produces RS devices with enhanced performance.

Finally, as a practical memory would need, we explored the possibility of switching the devices between high and low resistance values by applying single pulses of fixed voltages. We chose voltages above the SET and RESET thresholds (i.e., ±5 V) observed in the *I-V* curves or HSLs. Surprisingly, we found that the switching efficiency (defined as the number of successful SETS and RESETS against the number of attempts) with these single pulses is rather low (between 15%–20%), so we developed a "semi-intelligent" protocol following ideas developed in [21]. Here, the protocol insists on pulsing with the same polarity (at fixed voltages of 4 V (SET) and −5 V (RESET)) until RS effectively takes place. With this modification, the switching efficiency can be raised up to 100%. Fig. 6(a) shows the commutation between high and low resistance states by applying this protocol for 130 times. Panels (b) and (c) show the number of pulses which were necessary to SET and RESET the sample.

IV. Conclusion

Ferromagnetic thin films of $La_{2/3}Ca_{1/3}MnO_3$ were shown to exhibit superior resistive switching characteristics when grown under low oxygen pressures and pulsed with millisecond time-width pulses. Sharp transitions between low and high resistance states suggest a low dispersion of the threshold for oxygen vacancies movement. Switching properties are strongly dependant on the compliance current used for producing the high to low transition. An ON/OFF ratio as high as 1000 was obtained for optimal conditions. Obtained results were discussed within the framework of mobile oxygen vacancies.

Though single pulses show a poor performance for switching, the use of an "intelligent" algorithm that allows repeated pulsing enables their reliable use as a memory device. Multifunctional ability is envisaged for these electrically controlled devices, as tunable spin polarized transport (i.e., colossal magnetoresistance) could be used to determine their baseline resistance.

Acknowledgment

This work was supported in part by UNSAM (Project SJ10/05), MINCYT (INNOVAR program), CONICET (PIP 047), and DUPONT—CONICET. The authors thank F. Saccone (FI-UBA) for the use of the PLD facility.

References

[1] A. Sawa, *Mater. Today*, vol. 11, p. 28, 2008.
[2] R. Waser *et al., Adv. Mater.*, vol. 21, pp. 2632–2663, 2009.
[3] M. J. Rozenberg, *Scholarpedia*, vol. 6, no. 4, p. 11414, 2011.
[4] D. B. Strukov *et al., MRS Bull.*, vol. 37, p. 108, 2012.
[5] J. J. Yang *et al., MRS Bull.*, vol. 37, p. 131, 2012.
[6] S. Jin *et al., Science*, vol. 264, p. 413, 1994.
[7] A. Asamitsu *et al., Nature*, vol. 388, p. 50, 1997.
[8] S. Q. Liu *et al., Appl. Phys. Lett.*, vol. 76, p. 2749, 2000.
[9] M. Quintero *et al., Appl. Phys. Lett.*, vol. 86, p. 242102, 2005.
[10] N. Das *et al., Phys. Rev. B*, vol. 78, p. 235418, 2008.
[11] C. Jooss *et al., Phys. Rev. B*, vol. 77, p. 132409, 2008.
[12] N. A. Tulina *et al., Europhys. Lett.*, vol. 56, p. 836, 2001.
[13] M. Quintero *et al., Phys. Rev. Lett.*, vol. 98, p. 116601, 2007.
[14] M. J. Rozenberg *et al., Phys. Rev. B*, vol. 81, p. 115101, 2010.
[15] D. B. Chrisey and G. K. Hubler, Eds., *Pulsed Laser Deposition on Thin Films*. New York, NY, USA: Wiley, 1994.
[16] V. R. Galakhov *et al., Phys. Rev. B*, vol. 65, p. 113102, 2002.
[17] Prellier *et al., Appl. Phys. Lett.*, vol. 75, p. 1446, 1999.
[18] Y. B. Nian *et al., Phys. Rev. Lett.*, vol. 98, p. 146403, 2007.
[19] D. S. Shang *et al., Phys. Rev. B*, vol. 73, p. 245427, 2006.
[20] M. Fujimoto *et al., Appl. Phys. Lett.*, vol. 91, p. 223504, 2007.
[21] F. Gomez Marlasca *et al., Appl. Phys. Lett.*, vol. 98, p. 123502, 2011.